



Franson Interference Generated by a Two-Level System

M. Peiris, K. Konthasinghe, and A. Muller*

Physics Department, University of South Florida, Tampa, Florida 33620, USA

(Received 13 September 2016; published 19 January 2017)

We report a Franson interferometry experiment based on correlated photon pairs generated via frequency-filtered scattered light from a near-resonantly driven two-level semiconductor quantum dot. In contrast to spontaneous parametric down-conversion and four-wave mixing, this approach can produce single pairs of correlated photons. We have measured a Franson visibility as high as 66%, which goes beyond the classical limit of 50% and approaches the limit of violation of Bell's inequalities (70.7%).

DOI: [10.1103/PhysRevLett.118.030501](https://doi.org/10.1103/PhysRevLett.118.030501)

Introduction.—Entanglement is perhaps the most intriguing of all physical phenomena, and was famously challenged by Einstein, Podolsky, and Rosen (EPR) in 1935 [1]. The EPR paradox led to Bell's inequalities [2] which have since been tested by numerous experiments [3] including recent “loophole-free” tests [4–6] that have conclusively demonstrated that entanglement cannot be explained using local hidden variable theories.

Most experiments have employed photons that are entangled in the energy and polarization degrees of freedom [7–10]. However, this method is known to be sensitive to polarization-mode dispersion in optical fibers [11]. As an alternative, entanglement in the time-energy basis may be employed, wherein quantum information is encoded in the arrival time of photons, and long-distance fiber transmission over 300 km is possible [12]. The approach of using time-energy entangled photons was first formulated by Franson, with photon pairs created in an atomic decay process and two unbalanced interferometers [13]. Franson-type experiments have stimulated a plethora of research activities and have been extensively used for Bell tests in quantum optics [14–16].

Today, entangled photon pairs for Franson experiments are primarily produced via spontaneous parametric down-conversion or four-wave mixing, following two main methods. In time-energy experiments [17,18], a nonlinear medium is pumped by a continuous monochromatic laser and emission times of the photons have an uncertainty equal to the coherence time of the pump laser. On the other hand, in time-bin experiments [14,19], a nonlinear medium is pumped by pulses that have previously passed through an unbalanced interferometer, leading to a “which-path” ambiguity in emission time. However, both methods provide a nondeterministic pair generation, leading to limitations on the accuracy and security of quantum communication.

Single-photon sources, based on single atoms, ions, impurity centers, and quantum dots (QDs) [20], have emerged as alternatives [21,22], emitting no more than a single pair during any given cascade decay. In particular, intense research efforts using InAs semiconductor QDs have enabled the generation of triggered photon pairs at

high rates and under an electric pump in a monolithic semiconductor chip with a high degree of polarization entanglement [23,24]. Recently it was shown that such a polarization entanglement can be converted into time-bin entanglement, with the polarization entanglement derived from the biexciton-exciton three-level system [25,26].

Here we explore the possibility of generating time-energy entanglement starting directly from a two-level QD. This approach does not require an exciton-biexciton system and avoids the complexities associated with a residual fine-structure splitting. Instead, it relies on a resonantly driven two-level system, the light scattered by which is frequency filtered. We have investigated the ways in which correlated photons can be obtained and measured Franson visibilities using a pair of folded Mach-Zehnder interferometers (MZIs). The highest visibilities obtained (66%) beat the classical limit and approach the visibility required to violate Bell's inequalities (70.7%). This method paves the way for producing single time-energy entangled photon pair sources that violate Bell's inequalities.

Correlated photon pairs from the Mollow triplet.—Resonance fluorescence, one of the most fundamental signatures of a resonant light-matter interaction, is generated when a two-level system is exposed to a near-resonant light field. Under strong continuous laser illumination, the resonance fluorescence spectrum consists of a “Mollow triplet” composed of one central peak at the laser frequency, and two other peaks appearing on each side of the central peak and separated from the latter by a frequency approximately equal to the generalized Rabi frequency [Fig. 1(a)] [27–30]. The emergence of these peaks may be viewed as a result of a cascade emission down a ladder of pairs of “dressed states” [31,32] and it is natural to investigate under which circumstances photon-photon correlations can be generated via such a cascade. The seminal work by Cohen-Tannoudji and Reynaud first showed experimentally that filters positioned to select opposite Mollow triplet sidebands under a laser detuning can produce such correlations from a strongly driven two-level atom [33]. Later theoretical work provided expressions for the associated correlation functions [31,32,34].

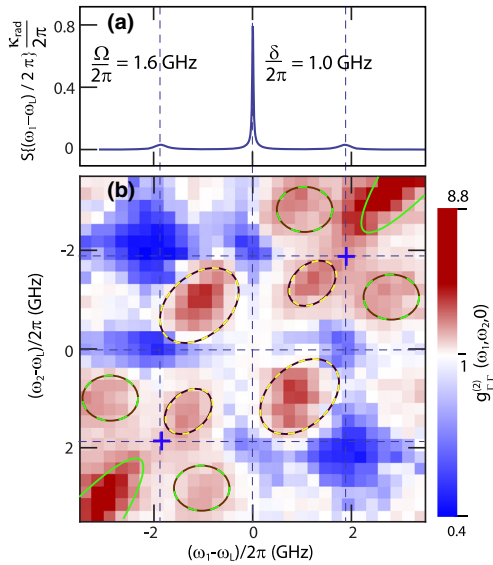


FIG. 1. (a) Theoretical one-photon spectrum (spectral density) for Rabi frequency $\Omega/2\pi = 1.6$ GHz and laser detuning $\delta/2\pi = 1.0$ GHz. (b) Experimental two-photon spectrum for the same parameters with filter bandwidths $\Gamma_1/2\pi = \Gamma_2/2\pi = \Gamma/2\pi = 0.45$ GHz. The recording time for each frequency pair on the 29×29 point grid was identical and equal to 165 s, which together with various delay times make the total measurement time of the map equal to about 42 hours.

Since then, bunching statistics have also been obtained for the case of a QD, with two Michelson interferometers selecting opposite sidebands in the Mollow triplet [35]. Recent theoretical work by del Valle *et al.* has reexamined the problem from a more general point of view and introduced the concept of a “two-photon spectrum” (TPS), $g_{\Gamma_1, \Gamma_2}^{(2)}(\omega_1, \omega_2, T_1, T_2)$, which measures the probability to detect one photon of frequency ω_1 at time T_1 and another photon of frequency ω_2 at time T_2 [36]. Using this concept, it was found that there are actually many ways that correlated photon pairs can be produced by spectrally filtering the scattered light from a resonantly excited two-level system [37].

In this work, QDs grown by molecular beam epitaxy were held in a free-space closed-cycle cryostat at a base temperature of 5 K [30]. While strongly driving a ground-state transition (neutral exciton) with a tunable continuous-wave laser (frequency ω_L), and using a perpendicular excitation and detection scheme [38], the resonance fluorescence from a single QD was obtained nearly background free with a collection efficiency into the first lens of order 10%. The radiative decay rate and spectral diffusion broadened linewidth were $\kappa_{\text{rad}}/2\pi = 0.2$ GHz and $\kappa_{\text{sd}}/2\pi \approx 1.0$ GHz, respectively. After splitting this QD scattered light into two equal parts, we introduced two stable filters [39], tunable both in their resonance frequencies (ω_1, ω_2) as well as in their bandwidths (Γ_1, Γ_2).

Figure 1(b) shows the experimental TPS for a Rabi frequency of $\Omega/2\pi = 1.6$ GHz, laser detuning, $\delta/2\pi = 1.0$ GHz, and filter bandwidths, $\Gamma_1/2\pi = \Gamma_2/2\pi = \Gamma/2\pi = 0.45$ GHz. Each point in the two-dimensional map represents the corresponding coincidence rate at $\tau = T_2 - T_1 = 0$ for a given filter frequency pair, which we have measured by histogramming the arrival times of photons.

While the scattered light from a two-level system has overall sub-Poissonian photon statistics, by selecting various frequency pairs one can distill different photon statistics as seen in Fig. 1(b) (red, super-Poissonian; blue, sub-Poissonian; and white, Poissonian). In particular, the TPS reveals that other than filtering opposite sidebands (blue crosses), one can generate correlated photon pairs also by filtering in-between Mollow triplet peaks (yellow-brown dashed contour), filtering opposite peak tails (solid green contour), or filtering an in-between Mollow triplet peak and an opposite peak tail (green-brown dashed contour). The latter features were identified as a family of “leapfrog” transitions through virtual states [40], though their exact origin is still being investigated [41]. Nonetheless, based on these correlations, violations of the Cauchy-Schwarz inequality have been predicted [42] and experimentally verified [37]. Moving one step further, to investigate the possibility of generating time-energy entanglement using QD resonance fluorescence, one can in principle use any filter frequency pair that can create correlated photon pairs [red region in Fig. 1(b)]. However, limitations imposed in part by the actual filter properties, and in part by the nonideality of the source, lead to a reduction of the actual parameter space under which Franson measurements can be performed with any given experimental apparatus. In general, a compromise must be found between the signal-to-noise ratio and the degree of correlation of the photon pairs. For this reason, the measurements presented below focus on the case of correlated photon pairs generated via frequency-filtered opposite sidebands in the presence of a modest laser detuning. Under these conditions, typical count rates are approximately $1 \times 10^4 \text{ s}^{-1}$ at each detector.

Franson interferometer.—The principle of the Franson interferometer is based on the superposition of two-photon events generated at different times [13]. The measurement apparatus consists of two unbalanced MZIs in which each MZI has a short arm of length S_i and a long arm of length L_i ($i = 1, 2$). If the optical path length difference ($\Delta L_i = L_i - S_i$) is less than the coherence length $c\tau_c$ of the incident photons, where τ_c is the photon coherence time and c is the speed of light, then one-photon interference will be visible as the length of an arm is varied. Therefore, to elicit two-photon interference in the coincidence detection between the detectors, ΔL has to be greater than $c\tau_c$.

For any incident photon pair, there are four equally probable ways to reach the detectors: both photons can take the long arms (L_1 and L_2), both may take the short

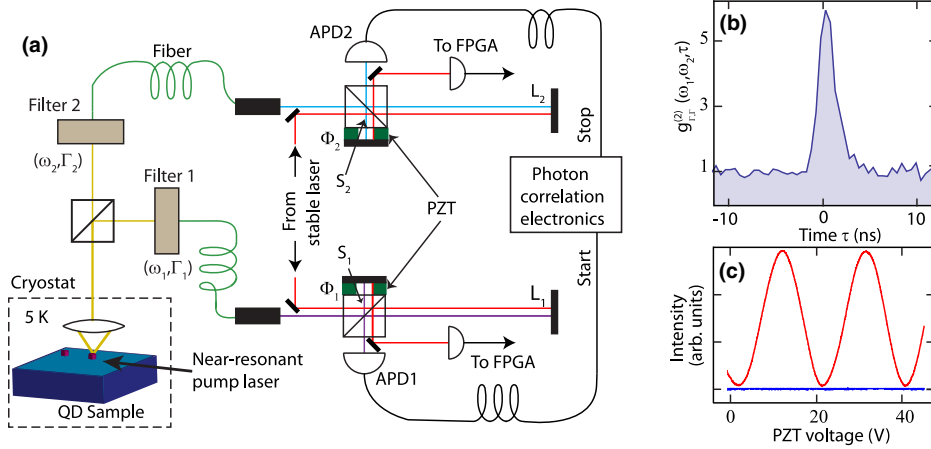


FIG. 2. (a) Experimental setup. The split frequency-filtered scattered light from a QD is connected to two unbalanced Mach-Zehnder interferometers, with $L_1 = L_2 = L = 190$ cm and $S_1 = S_2 = S = 2$ cm. The phase of each interferometer (Φ_i) is controlled by varying the length of their respective short arms. (b) Second-order correlation function for $\Omega/2\pi = 1.6$ GHz, $\delta/2\pi = 1.2$ GHz, $(\omega_1 - \omega_L)/2\pi = -(\omega_2 - \omega_L)/2\pi = 2.0$ GHz. (c) One-photon interference (95%) observed at each interferometer during the alignment process, using the pump laser as the interferometer input. The blue line denotes the background level.

arms (S_1 and S_2), or one photon may take the short (S_1) while the other takes the long arm (L_2) and vice versa. If $L_1 = L_2$ and $S_1 = S_2$, then these four possible paths will appear as three distinct peaks in a coincidence measurement. The first two cases are indistinguishable in their time of detection, as long as the path length difference in both interferometers is kept smaller than the coherence length of the pump laser. The last two events are distinguishable from each other as well as from the first two cases because of the delay between “clicks” of the two detectors; i.e., the detector receiving the photon taking the short path will “click” first. Note that the distinction of events is achieved by postselection of recorded time tags. The two-photon interference effect in indistinguishable events is a manifestation of photon entanglement in time, and a time-energy entangled state can be written as $|\Phi\rangle = (1/\sqrt{2})(|S_1, S_2\rangle + e^{i(\Phi_1 + \Phi_2)}|L_1, L_2\rangle)$, where $\Phi_1 = \Phi_{L_1} - \Phi_{S_1}$ and $\Phi_2 = \Phi_{L_2} - \Phi_{S_2}$ are the phase differences between the respective long and short arms in the interferometers.

Results.—The implementation of Franson interferometry using the light scattered from a QD is illustrated in Fig. 2(a). Frequency-filtered resonance fluorescence was sent directly into a MZI formed by a nonpolarizing 50:50 beam splitter and two mirrors. The optical path length difference in each interferometer was about 188 cm ($S = 2$ cm and $L = 190$ cm), which is much larger than the coherence length ($c\tau_c \approx 30$ cm) of the photons scattered by an InAs QD [43]. Filter frequencies were set in such a way as to generate correlated photon pairs under the conditions $\Omega/2\pi = 1.6$ GHz, $\delta/2\pi = 1.2$ GHz, and $(\omega_1 - \omega_L)/2\pi = -(\omega_2 - \omega_L)/2\pi = 2.0$ GHz, with the correlation function shown in Fig. 2(b). A piezoelectric transducer (PZT) was used to vary the relative phase, Φ , between the short and long arms in the interferometers, which were carefully

aligned with the pump laser to obtain a high degree (95%) of one-photon interference [Fig. 2(c)]. Finally, the output of each interferometer was connected to a single-photon counting detector (APD1 and APD2) with a time resolution of less than 500 ps. The normalized coincidence rate between the two detectors is shown in Fig. 3 for two phase adjustments. Figures 4(a) and 4(b) show the phase-dependent normalized coincidences within the central peak for a time window of 1024 and 4096 ps, respectively.

For a source of strongly correlated photon pairs, the total number of coincidences in the middle peak in Fig. 3 undergoes interference while the phases of the interferometers (Φ_1 and Φ_2) are varied. The phases for the measurements reported in Figs. 3(a) and 3(b) were such that the middle peak was minimized and maximized, respectively.

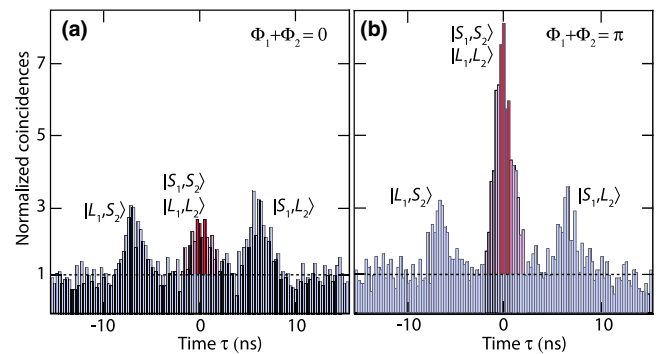


FIG. 3. Histograms of the normalized coincidence rate for two different phase settings as indicated, (a) minimizing and (b) maximizing the central peak. The measurement time was 600 s for each panel and the bin width was 256 ps. The red and pink shaded areas indicate the coincidences involved in the calculation of the visibility as defined in the text. The dashed black line indicates the accidentals level.

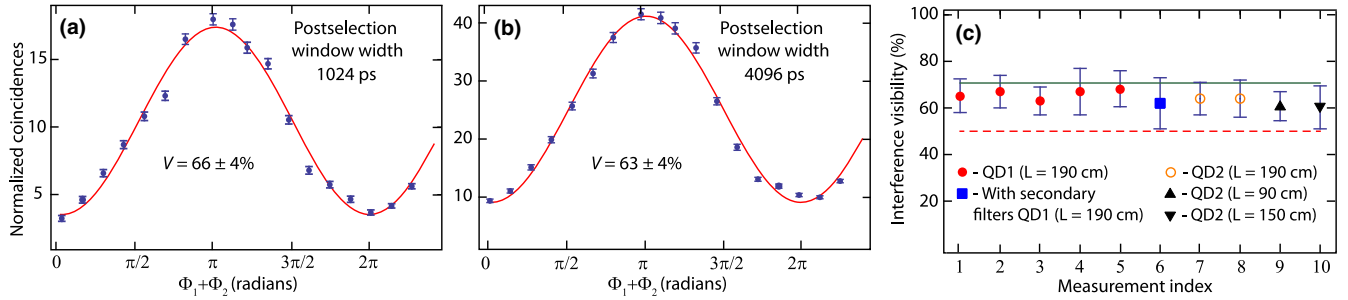


FIG. 4. Normalized coincidences in the central peak plotted as a function of the phase $\Phi_1 + \Phi_2$ with a postselection window width of (a) 1024 ps and (b) 4096 ps. (c) Franson visibilities for different measurement settings. The red dashed line and the green solid line indicate the classical limit (50%) and the limit at which Bell's inequalities are violated (70.7%), respectively.

The height of the side peaks were found to be independent of the phases. For this particular measurement the total recording time was 600 s and the bin size was 256 ps. An interference visibility can be defined in the usual way as $V = (C_{\max} - C_{\min}) / (C_{\max} + C_{\min})$, where C_{\min} (C_{\max}) are the number of coincidences, above the accidentals level, associated with the middle peak under interference minimum (maximum) conditions. By postselecting events occurring within a 1024-ps-wide time window (approximately coinciding with the coherence time of QD scattered photons) (red bars in Fig. 3) and while changing the phases of the interferometers (Φ_1 and Φ_2), we have obtained a visibility of $V = 66\% \pm 4\%$ after fitting with a sinusoidal function [Fig. 4(a)], which exceeds the classical limit (50%) and is close to the limit corresponding to a violation of Bell's inequalities (70.7%) [44]. For a larger time window of 4096 ps (combination of the red and pink bars in Fig. 3), a visibility of $63\% \pm 4\%$ [Fig. 4(b)] was obtained.

Discussion.—Ideally, the visibility in this experiment would be equal to unity, and we have investigated the potential causes for the imperfect interference seen in Figs. 3 and 4. An essential requirement in Franson's scheme is that $c\tau_p \gg \Delta L$ [13], where τ_p is the pump laser coherence time. We have used a stable continuous-wave pump laser with a coherence time of about 166 ns ($\Delta L/c \approx 6$ ns), thus meeting this requirement. The same laser was used to align the MZIs, and its long coherence time is confirmed by the high degree of one-photon interference ($\approx 95\%$) in Fig. 2(c). To ensure that the visibility was not artificially reduced by random phase fluctuations in the MZIs, we employed an active stabilization method [Fig. 2(a)] consisting of a stable secondary laser and field-programmable gate array (FPGA) controllers providing feedback to the PZTs [45]. Moreover, by carefully fiber coupling the output of each interferometer using free-space lenses, we have verified that the contributions from the two arms of each interferometer are within 2% of each other, which resulted in similar probabilities for “long-long” and “short-short” coincidence events. This leaves the possibility of intrinsic nonidealities associated with the source, and/or limitations originating in the filters

we employed. To verify the integrity of our filtering process, we have repeated the experiment in the presence of an additional prefilter [Fig. 4(c) measurement 6], which increased the off-resonance rejection ratio. However, we found no significant influence of this prefilter on the final Franson visibility. It is thus very likely that the nonunity Franson visibility observed here has its origin in the source itself; further investigations will be needed to draw additional conclusions. We note nonetheless that we could not observe a significant variation in visibility when performing the experiment for different QDs in the same sample [Fig. 4(c) measurements 7–10].

Conclusion.—We have used two-photon interference obtained from a Franson interferometer to investigate the possibility of generating time-energy entanglement using a resonantly driven two-level system, the scattered light from which was spectrally filtered. The measured Franson visibility of 66% indicates a clear violation over the classical limit and approaches the limit for a violation of Bell's inequalities. We speculate that the visibility in our experiments is limited by properties intrinsic to the source, perhaps originating in influences related to phonon scattering and/or spectral diffusion, which are processes often causing deviations from ideal two-level system behavior in InAs epitaxial QDs [30,46,47]. Nonetheless, our method based on single-photon pairs can be potentially used in future quantum communication schemes, with entanglement preserved through optical fibers.

The authors acknowledge financial support from the National Science Foundation (NSF Grant No. 1254324).

*mullera@usf.edu

- [1] A. Einstein, B. Podolsky, and N. Rosen, *Phys. Rev.* **47**, 777 (1935).
- [2] J. S. Bell, *Physics* (Long Island City, N.Y.) **1**, 195 (1964).
- [3] A. Aspect, P. Grangier, and G. Roger, *Phys. Rev. Lett.* **49**, 91 (1982).
- [4] B. Hensen *et al.*, *Nature* (London) **526**, 682 (2015).
- [5] M. Giustina *et al.*, *Phys. Rev. Lett.* **115**, 250401 (2015).
- [6] L. K. Shalm *et al.*, *Phys. Rev. Lett.* **115**, 250402 (2015).

- [7] A. K. Ekert, *Phys. Rev. Lett.* **67**, 661 (1991).
- [8] D. Boschi, S. Branca, F. De Martini, L. Hardy, and S. Popescu, *Phys. Rev. Lett.* **80**, 1121 (1998).
- [9] T. Jennewein, C. Simon, G. Weihs, H. Weinfurter, and A. Zeilinger, *Phys. Rev. Lett.* **84**, 4729 (2000).
- [10] D. S. Naik, C. G. Peterson, A. G. White, A. J. Berglund, and P. G. Kwiat, *Phys. Rev. Lett.* **84**, 4733 (2000).
- [11] M. Brodsky, E. C. George, C. Antonelli, and M. Shtaif, *Opt. Lett.* **36**, 43 (2011).
- [12] T. Inagaki, N. Matsuda, O. Tadanaga, M. Asobe, and H. Takesue, *Opt. Express* **21**, 23241 (2013).
- [13] J. D. Franson, *Phys. Rev. Lett.* **62**, 2205 (1989).
- [14] J. Brendel, N. Gisin, W. Tittel, and H. Zbinden, *Phys. Rev. Lett.* **82**, 2594 (1999).
- [15] D. Grassani, S. Azzini, M. Liscidini, M. Galli, M. J. Strain, M. Sorel, J. E. Sipe, and D. Bajoni, *Optica* **2**, 88 (2015).
- [16] R. Wakabayashi, M. Fujiwara, K. Yoshino, Y. Nambu, M. Sasaki, and T. Aoki, *Opt. Express* **23**, 1103 (2015).
- [17] W. Tittel, J. Brendel, N. Gisin, and H. Zbinden, *Phys. Rev. A* **59**, 4150 (1999).
- [18] I. A. Khan and J. C. Howell, *Phys. Rev. A* **73**, 031801(R) (2006).
- [19] I. Marcikic, H. de Riedmatten, W. Tittel, V. Scarani, H. Zbinden, and N. Gisin, *Phys. Rev. A* **66**, 062308 (2002).
- [20] J.-M. Gérard and B. Gayral, *J. Lightwave Technol.* **17**, 2089 (1999).
- [21] C. Simon and J.-P. Poizat, *Phys. Rev. Lett.* **94**, 030502 (2005).
- [22] P. K. Pathak and S. Hughes, *Phys. Rev. B* **83**, 245301 (2011).
- [23] R. M. Stevenson, R. J. Young, P. Atkinson, K. Cooper, D. A. Ritchie, and A. J. Shields, *Nature (London)* **439**, 179 (2006).
- [24] A. Muller, W. Fang, J. Lawall, and G. S. Solomon, *Phys. Rev. Lett.* **103**, 217402 (2009).
- [25] H. Jayakumar, A. Predojević, T. Kauten, T. Huber, G. S. Solomon, and G. Weihs, *Nat. Commun.* **5**, 4251 (2014).
- [26] M. A. M. Versteegh, M. E. Reimer, A. A. van den Berg, G. Juska, V. Dimastrodonato, A. Gocalinska, E. Pelucchi, and V. Zwiller, *Phys. Rev. A* **92**, 033802 (2015).
- [27] B. R. Mollow, *Phys. Rev.* **188**, 1969 (1969).
- [28] E. B. Flagg, A. Muller, J. W. Robertson, S. Founta, D. G. Deppe, M. Xiao, W. Ma, G. J. Salamo, and C. K. Shih, *Nat. Phys.* **5**, 203 (2009).
- [29] S. Ates, S. M. Ulrich, S. Reitzenstein, A. Löffler, A. Forchel, and P. Michler, *Phys. Rev. Lett.* **103**, 167402 (2009).
- [30] K. Konthasinghe, J. Walker, M. Peiris, C. K. Shih, Y. Yu, M. F. Li, J. F. He, L. J. Wang, H. Q. Ni, Z. C. Niu, and A. Muller, *Phys. Rev. B* **85**, 235315 (2012).
- [31] A. Aspect, G. Roger, S. Reynaud, J. Dalibard, and C. Cohen-Tannoudji, *Phys. Rev. Lett.* **45**, 617 (1980).
- [32] G. Nienhuis, *Phys. Rev. A* **47**, 510 (1993).
- [33] C. Cohen-Tannoudji and S. Reynaud, *Phil. Trans. R. Soc. A* **293**, 223 (1979).
- [34] C. A. Schrama, G. Nienhuis, H. A. Dijkerman, C. Steijsiger, and H. G. M. Heideman, *Phys. Rev. A* **45**, 8045 (1992).
- [35] A. Ulhaq, S. Weiler, S. M. Ulrich, R. Roßbach, M. Jetter, and P. Michler, *Nat. Photonics* **6**, 238 (2012).
- [36] E. del Valle, A. Gonzalez-Tudela, F. P. Laussy, C. Tejedor, and M. J. Hartmann, *Phys. Rev. Lett.* **109**, 183601 (2012).
- [37] M. Peiris, B. Petrak, K. Konthasinghe, Y. Yu, Z. C. Niu, and A. Muller, *Phys. Rev. B* **91**, 195125 (2015).
- [38] A. Muller, E. B. Flagg, P. Bianucci, X. Y. Wang, D. G. Deppe, W. Ma, J. Zhang, G. J. Salamo, M. Xiao, and C. K. Shih, *Phys. Rev. Lett.* **99**, 187402 (2007).
- [39] B. Petrak, M. Peiris, and A. Muller, *Rev. Sci. Instrum.* **86**, 023104 (2015).
- [40] A. Gonzalez-Tudela, F. P. Laussy, C. Tejedor, M. J. Hartmann, and E. del Valle, *New J. Phys.* **15**, 033036 (2013).
- [41] V. N. Shatokhin and S. Y. Kilin, *Phys. Rev. A* **94**, 033835 (2016).
- [42] C. Sánchez Muñoz, E. del Valle, C. Tejedor, and F. P. Laussy, *Phys. Rev. A* **90**, 052111 (2014).
- [43] P. Borri, W. Langbein, S. Schneider, U. Woggon, R. L. Sellin, D. Ouyang, and D. Bimberg, *Phys. Rev. Lett.* **87**, 157401 (2001).
- [44] J. G. Rarity and P. R. Tapster, *Phys. Rev. Lett.* **64**, 2495 (1990).
- [45] A. Schwettmann, J. Sedlacek, and J. P. Shaffer, *Rev. Sci. Instrum.* **82**, 103103 (2011).
- [46] J. Förstner, C. Weber, J. Danckwerts, and A. Knorr, *Phys. Rev. Lett.* **91**, 127401 (2003).
- [47] A. V. Kuhlmann, J. H. Prechtel, J. Houel, A. Ludwig, D. Reuter, A. D. Wieck, and R. J. Warburton, *Nat. Commun.* **6**, 8204 (2015).